Amorphous phase separation in the metallic glasses $(Pb_{1-y}Sb_y)_{1-x}Au_x$

C. O. Kim and W. L. Johnson
W. M. Keck Laboratory of Engineering Materials, California Institute of Technology, Pasadena, California 91125
(Received 17 June 1980)

A novel family of ternary superconducting metallic glasses of the form $(Pb_{1-y}Sb_y)_{1-x}Au_x$ have been prepared by the method of melt quenching and studied by x-ray diffraction and electron microscopy. For $y=0.5$ and 0.25, and $0.35<x<0.7$, measurements of superconducting properties suggest that these glasses are phase separated into two amorphous phases. X-ray-diffraction studies also suggest a phase separation. The two amorphous phases have been directly observed using electron microscopy and selected area electron diffraction. The scale of the domain structure is 1000–2000 Å. All of the superconducting properties measured can be understood in terms of the observed separation of amorphous phases.

I. INTRODUCTION

The first evidence of phase separation in metallic glasses was reported by Chen and Turnbull.[1] On the basis of small-angle x-ray-scattering experiments, they concluded that the metallic glass $Pd_{74}Au_8Si_{18}$ undergoes a phase separation into two glass phases at a sufficiently high temperature. Such a phase separation can be understood by comparison with the case of spinodal decomposition in metastable crystalline solid solutions. A sound theoretical treatment of this problem has been given by Cahn.[2] In a binary alloy a single-phase solid solution lying within the spinodal boundary is unstable against decomposition into two phases of differing composition. The existence of a spinodal region requires a positive heat of mixing of two constituents phases in some region of the binary phase diagram.

In the present study, we have examined the problem of phase separation in a series of ternary metallic glasses of the form $(Pb_{1-y}Sb_y)_{1-x}Au_x$. These glasses were prepared by rapid cooling from the liquid state using techniques described elsewhere.[3] Both the "gun technique" and the "piston and anvil technique" were used. All of these glassy alloys were found to be superconducting. By studying the variation of superconducting properties with alloy composition, it was possible to clearly identify composition ranges for which phase separation had occurred. Investigation of the structure and morphology of these samples using x-ray-diffraction techniques together with electron microscopy confirmed the existence of phase separation in the range of compositions studied.

II. EXPERIMENTAL RESULTS

Samples were first prepared using the "gun technique." The samples were quenched onto a copper substrate maintained at a temperature of 77 K by immersing one end of the substrate in liquid nitrogen. The samples were kept in liquid nitrogen following the quench and transferred to a cold-finger assembly attached to a Norelco diffractometer where preliminary x-ray-diffraction patterns were obtained. The sample could be maintained at a temperature of $T \approx 200$ K with this arrangement. Based on these diffraction scans, a metastable ternary phase diagram was determined. This diagram is shown in Fig. 1. The figure shows that a broad range of ternary compositions exist for which an amorphous phase is obtained. Note that no binary amorphous alloys were obtained.

Next, the samples were allowed to warm up to room temperature. After a period of one hour, the x-ray-diffraction scans were repeated. Evidence of crystallization was found in some of the samples. In particular, those samples lying near the boundary of

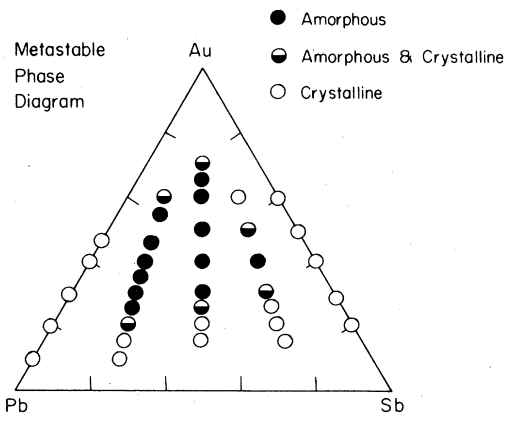

FIG. 1. Metastable ternary phase diagram showing regions of the Pb-Sb-Au system which form a metallic glass under rapid quenching conditions (cooling rate of $\sim 10^6$ °C/sec). Some of the alloys were quenched onto substrates cooled by liquid nitrogen as discussed in the text.

the amorphous phase range in Fig. 1 had partially crystallized at room temperature. On the other hand, several of the amorphous alloys did not crystallize. In particular, samples with $y = 0.25$ and 0.50 and $0.35 \leq x \leq 0.70$ did not crystallize. These compositions were chosen for further studies.

The "piston and anvil" method with a room-temperature substrate was then used to produce foils of those alloys found to be stable against crystallization at room temperature on a practical time scale. The foils produced have an area of several cm^2 and a thickness of about 40 μm. Amorphous alloys of composition $(Pb_{1-y}Sb_y)_{1-x}Au_x$ with $y = 0.5$ and $x = 0.4$, 0.5, 0.6, and 0.7 were found to be initially amorphous and stable against crystallization at room temperature. The x-ray scans were repeated at intervals of several days on these specimens. No evidence of crystallization was observed for a period of several weeks in those samples with $0.40 \leq x \leq 0.70$.

Inductive and resistive measurements of the superconducting transition temperature were made both on "gun-quenched" samples and "piston and anvil"-quenched samples. Again, care was taken to ensure that the gun quenched samples were maintained at low temperature by transferring the samples to the probe under liquid nitrogen. This precaution was taken to avoid possible crystallization of the less stable samples. The electrical resistance as a function of temperature was measured using a standard four-point probe technique. Sharp superconducting transitions were observed in most samples. A summary of results is shown in Fig. 2. The superconducting transition temperature was taken to be the midpoint of the resistive transition. The transition temperature is plotted as a function of composition for the two alloy series $(Pb_{0.75}Sb_{0.25})_{1-x}Au_x$ and $(Pb_{0.5}Sb_{0.5})_{1-x}Au_x$ in Fig. 3. An obvious change in the slope of the T_c vs x curve was observed in both alloy series as can be seen in the figure. This will be discussed in Sec. III.

The upper critical field H_{c2} was measured for the alloy series $(Pb_{0.5}Sb_{0.5})_{1-x}Au_x$ using samples prepared by both techniques. The critical field was determined by plotting the resistance of the sample as a function of applied field at constant temperature. The field was applied normal to the direction of current flow and was produced by a superconducting NbTi solenoid. Again, the midpoint of the resistive transition was used to define H_{c2}. The results obtained were very similar for samples of the same composition prepared by the two different methods. For clarity, only the results for a series of $(Pb_{0.5}Sb_{0.5})_{1-x}Au_x$ samples prepared by the piston and anvil method are presented. The temperature dependence of H_{c2} is shown for this alloy series in Fig. 4. For those samples with Au content $x > 0.4$, the H_{c2} curves show two distinct regions of behavior. The curves are linear at high temperature but show an abrupt change in slope at a lower temperature. This behavior will be interpreted in Sec. III.

A detailed x-ray-diffraction study was carried out for samples of the $(Pb_{0.5}Sb_{0.5})_{1-x}Au_x$ series with

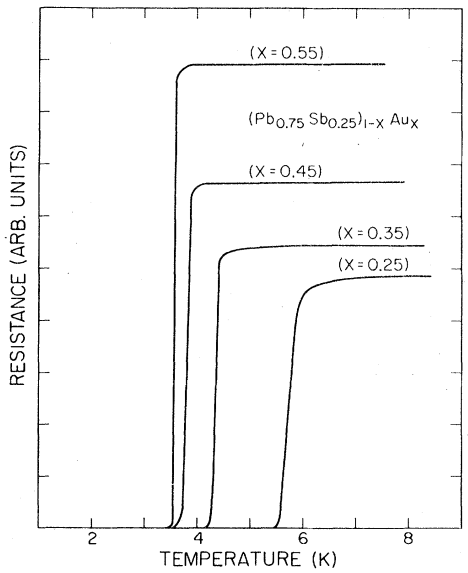

FIG. 2. Electrical resistance (arbitrary units) as a function of temperature showing superconducting transitions for several $(Pb_{1-y}Sb_y)_{1-x}Au_x$ alloys.

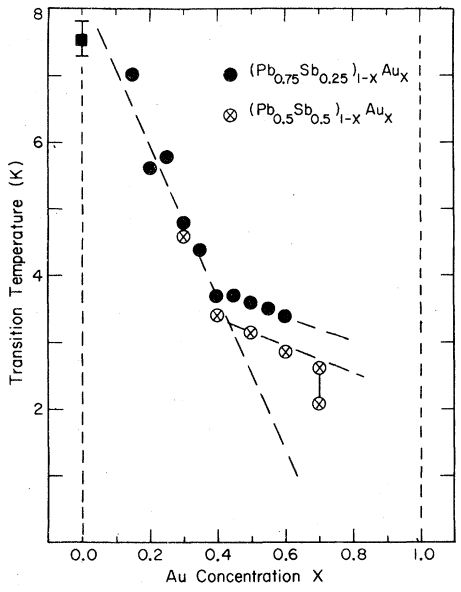

FIG. 3. Superconducting transition temperature as a function of composition for the two alloy series $(Pb_{0.75}Au_{0.25})_{1-x}Au_x$ and $(Pb_{0.5})_{1-x}Au_x$. The two points shown for $x = 0.70$ are the T_c's of the two separated phases as determined by application of a magnetic field. This is discussed in the text.

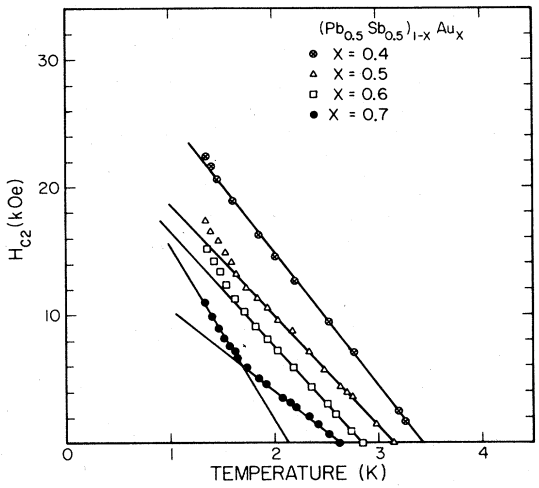

FIG. 4. Upper critical field $H_{c2}(T)$ for a series of $(Pb_{0.5}Sb_{0.5})_{1-x}Au_x$ alloys.

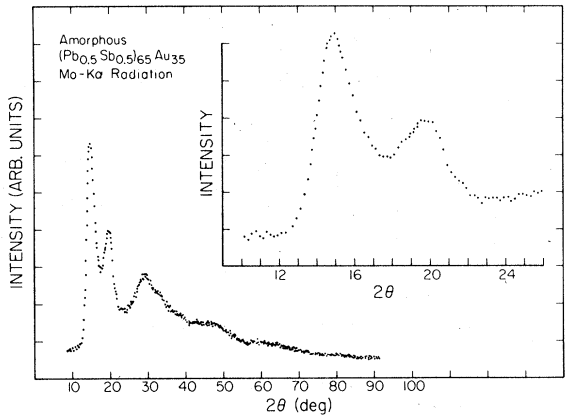

FIG. 5. X-ray-scattering intensity as a function of scattering angle for amorphous $(Pb_{0.5}Sb_{0.5})_{0.65}Au_{0.35}$.

$0.35 \leq x \leq 0.70$. The foils studied were those prepared by the piston and anvil technique. For $x < 0.35$, the samples began to crystallize during the scans which were taken over a period of 24 h. The diffraction stage was enclosed in a vacuum chamber and the specimen could be cooled to approximately $T = 200$ K by mounting it on a cold finger. A horizontal Mylar window of thickness 0.002 in. was used to allow x rays to pass in and out of the chamber. The entire sample stage was mounted on a GE scanning goniometer using Zr-filtered Mo $K\alpha$ x-ray radiation. A diffracted beam monochromator was used to eliminate inelastically scattered x rays. The diffraction patterns were obtained by step scanning with counting intervals of 150 sec. Typical results are shown in Figs. 5 and 6 for the alloy compositions $x = 0.35$ and 0.55. The most striking feature of the x-ray patterns is the clear splitting of the first diffraction maximum into two submaxima. This splitting was observed in all alloys with $0.35 \leq x \leq 0.70$. For alloys with $x = 0.20$ and 0.25 the second submaxima did not seem to be present. However, evidence of crystallization (sharp Bragg peaks) was already present before the x-ray scanning had progressed completely through the region of interest. A rough x-ray scan was taken over a 20 min period and showed no evidence of the second submaxima in the $x = 0.20$ sample. It is thus clear that the relative height of the second submaximum increases with increasing x for $x \geq 0.35$ while this maxima appears to disappear entirely for $x \sim 0.20$.

In order to further study the above splitting of the first maxima, electron microscopy and diffraction were carried out on samples of the composition $(Pb_{0.5}Sb_{0.5})_{0.45}Au_{0.55}$. The foils were thinned by etching with a (30–70%) mixture of perchloric and acetic acid. The electron microscopy revealed that the etching process was nonuniform with the etch preferentially attacking selected regions of the sample and leaving an obvious domain structure with domain sizes of about 1000–2000 Å. A micrograph showing these domains is presented in Fig. 7. The light areas are thinner than the dark areas due to preferential etching. Selected area electron diffraction patterns were taken in each of these regions as shown in the figure. The diffraction pattern in each domain type was found to exhibit a single first diffraction maximum. The diameter of this maxima changed abruptly on moving the beam from one region to the other as shown in Fig. 8. This shows conclusively that the alloy is phase separated and that the two submaxima observed in x-ray diffraction arise in fact from separate amorphous phases. Direct comparison of

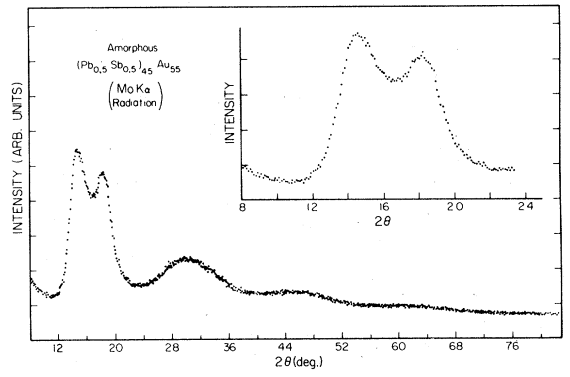

FIG. 6. X-ray-scattering intensity as a function of scattering angle for amorphous $(Pb_{0.5}Sb_{0.5})_{0.45}Au_{0.55}$. Arrows show positions of diffraction maxima corresponding to Pb–Pb (Sb–Pb or Sb–Sb) neighbors and Au–Au neighbors as discussed in the text. These are labeled Pb and Au, respectively.

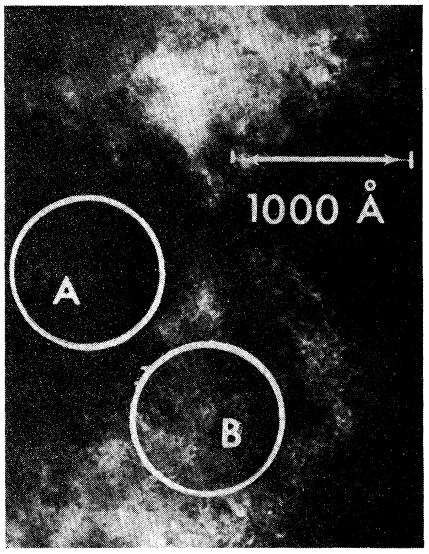

FIG. 7. Electron micrograph of a typical region in a chemically thinned specimen of $(Pb_{0.5}Sb_{0.5})_{0.45}Au_{0.55}$. Domain structure is clearly visible.

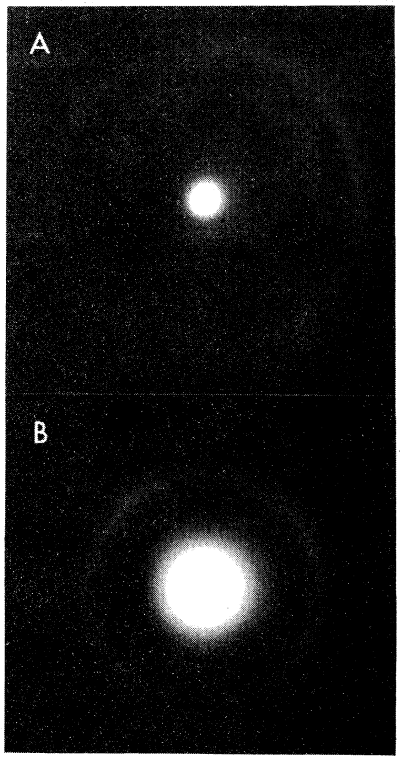

FIG. 8. Transmission electron diffraction patterns for selected regions of micrograph shown in Fig. 7. Regions are indicated in Fig. 7.

the magnitude of the scattering vectors which characterize the diffraction maxima can be made. In electron diffraction we find $K_{max}^{ed} = 2.21$ Å^{-1} and 2.85 Å^{-1} (± 0.05 Å^{-1}) for the patterns shown in Fig. 8. For the corresponding x-ray-diffraction pattern (Fig. 6) we obtain $K_{max}^{xd} = 4\pi \sin\theta_{max}/\lambda = 2.24$ Å^{-1} and 2.80 Å^{-1} (± 0.01 Å^{-1}), respectively, for the two submaxima where $2\theta_{max}^{xd} = 14.55°$ and 18.20°, respectively. The x-ray and electron diffraction give values of K_{max}, which are in good agreement. Thus we have made a clear identification of two amorphous phases.

In order to fully characterize the structure of the two amorphous phases observed, we would need a detailed diffraction pattern for each separate phase. This in turn could be Fourier transformed to obtain the separate pair-correlation function $G(r)$ for each phase. This is beyond the scope of the present study. On the other hand, one can obtain a rough estimate of the typical distance between nearest-neighbor atoms in an amorphous alloy from the position K_{max} of the first maximum of the diffraction pattern of the alloy by using the Debye formula.[4,5] This formula relates the position of the first diffraction maxima to the dominant period of spatial oscillation in the corresponding $G(r)$. The spatial period is given by[4]

$$d \approx \frac{1.23\lambda}{2\sin\theta_{max}} = \frac{1.23(2\pi)}{K_{max}} .$$

Using the K_{max} values from x-ray diffraction gives $d_1 \approx 3.45$ Å and $d_2 \approx 2.76$ Å for the two submaxima. Crudely speaking, d is a rough estimate of the typical first-nearest-neighbor distance in amorphous metallic alloys. The metallic radii of Pb, Sb, and Au are $r_m = 1.75$, 1.59, and 1.44 Å, respectively. The sum of two Au radii gives 2.88 Å whereas any other sum of two radii gives a value in the range 3.03–3.5 Å. On this basis, one can speculate that the distance $d_2 = 2.76$ Å would most likely correspond to neighboring Au atoms. This in turn would suggest that the second maximum (in Fig. 6) at $2\theta = 18.20°$ (which corresponds to d_2) is associated with a Au-rich phase. The observed phase separation would then involve a Au-rich and Au-poor phase. The disappearance of the second submaximum at low-Au concentration ($x = 0.20$) would then imply that these Pb,Sb-rich alloys are single phase. This above argument should, nevertheless be treated with some caution since the Debye formula does not always yield accurate nearest-neighbor distances.

III. DISCUSSION AND INTERPRETATION

The results of Fig. 3 suggest that superconductivity is dominated by one phase for Au concentrations up to $x \approx 0.35$ in the $(Pb_{0.5}Sb_{0.5})_{1-x}Au_x$ and $(Pb_{0.75}Sb_{0.25})_{1-x}Au_x$ alloys. The change in slope in the T_c vs x curve near this concentration can be un-

derstood by assuming that alloys with $x \geq 0.4$ contain significant amounts of two superconducting phases. One phase, with Au content $x \approx 0.40$ has a superconducting transition temperature $T_c \approx 3.2$ K and remains present in alloys with $x \geq 0.4$. Since the scale of phase separation ($\sim 1000-2000$ Å) is large compared with the superconducting coherence length of this phase, no appreciable degradation of the T_c of this phase should occur as a result of the proximity effect.[6] The H_{c2} curve (Fig. 4) of the $(Pb_{0.5}Sb_{0.5})_{0.6}Au_{0.4}$ sample has a single slope which can be used to estimate the coherence length of the associated superconducting phase using the relation

$$\xi(T) = \left[\frac{\phi_0}{2\pi H_{c2}}\right]^{1/2} .$$

A linear least-squares fit to the data yields $H_{c2}(T) = 10.5(T_c - T)(\text{kOe})$ which in turn gives

$$\xi(T) = \left[\frac{T_c}{T_c - T}\right]^{1/2} (94\ \text{Å}) ,$$

where $T_c = 3.24$ K. This gives an estimated $\xi(0) = 94$ Å which is more than an order of magnitude smaller than the domain size (1000–2000 Å). This verifies the assertion that the proximity effect should not degrade the transition temperature of the high T_c phase. The presence of a phase with Au content $x \approx 0.40$ in alloys with $x > 0.40$ should result in a nearly constant T_c with increasing x. In other words, the superconducting properties for two-phase alloys with average Au content $x > 0.4$ are governed by a Au-poor phase with $x \approx 0.40$. This is exactly what is observed in the variation of T_c with x (Fig. 3). T_c is much less dependent on composition for $x > 0.40$.

The H_{c2} curves in Fig. 4 yield additional information. As x increases above 0.4, the H_{c2} curves develop two branches. At $x = 0.7$, this effect is very pronounced. One can explain these results by assuming that the two phases found in x-ray and electron diffraction have different intrinsic upper critical-field gradients $(dH_{c2}/dT)_{T_c}$ as well as different T_c values. For example, in the case of $x = 0.7$, one phase with $T_c \approx 2.7$ K and $(dH_{c2}/dT) \approx 7$ kOe/K and a second phase with $T_c \approx 2.1$ K and $(dH_{c2}/dT) \approx 12$ kOe/K will account for the observed behavior of H_{c2}. According to the above argument, the high T_c phase is presumably rich in (Pb,Sb) while the low T_c phase contains a higher Au concentration. Both T_c's were plotted in Fig. 3 for comparison. The use of the magnetic field allows the properties of both phases to be separately estimated.

The simple picture used here to interpret the superconducting properties of these alloys assumes two phases of uniform composition. In the case of a spinodal decomposition process, a concentration gradient will exist and this simple picture will not be exact. The qualitative features described should nevertheless persist. The anomalous behavior of the $T_c(x)$ and $H_{c2}(T)$ curves could still be understood as being due to phase separation. The exact nature of the decomposition process in the present alloys is not known. Studies are presently in progress aimed at determining the exact composition of each phase in the phase separated alloys. A study of the corresponding liquid alloys is also being carried out.

Finally, it is also important to point out that the kinetics of phase separation have not been addressed in this article. It is not known, for example, whether phase separation occurs in the liquid alloy before quenching, during the quenching process, or following the quench. The comparative instability of these materials at room temperature make a systematic study of kinetics difficult. As such, direct information regarding the temperature dependence of the phase-separation process must await further studies.

ACKNOWLEDGMENTS

One of the authors (C.O.K.) wishes to thank the Korean Ministry of Education for providing support for his stay at Caltech. This work was carried out under contract for the U.S. DOE Contract No. DE-AC03-76ER00822.

[1]C. P. Chou and D. Turnbull, J. Non-Cryst. Solids 17, 169 (1975).

[2]J. W. Cahn, Acta Metall. 4, 217 (1956); 7, 18 (1959); 9, 795 (1961).

[3]P. Duwez, *Progress in Solid State Chemistry* (Pergamon, Oxford, 1966), Vol. 3.

[4]See for example, A. Guinier, *X-ray Diffraction* (Freeman, San Francisco, 1963), Chap. 3, p. 72.

[5]G. S. Cargill, III, Solid State Phys. 30, 227 (1975).

[6]G. Deveschер and P. G. de Gennes, in *Superconductivity*, edited by R. D. Parks (Marcel Dekker, New York, 1969), p. 1005.

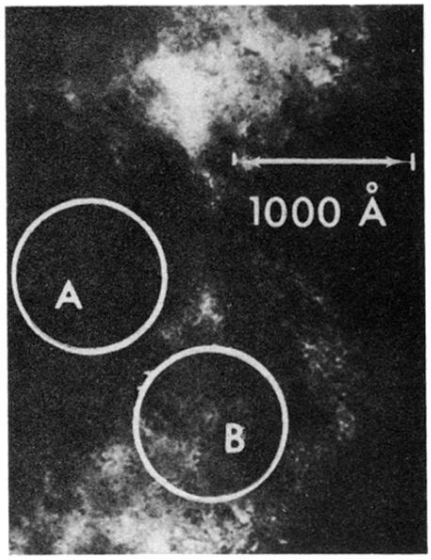

FIG. 7. Electron micrograph of a typical region in a chemically thinned specimen of $(Pb_{0.5}Sb_{0.5})_{0.45}Au_{0.55}$. Domain structure is clearly visible.

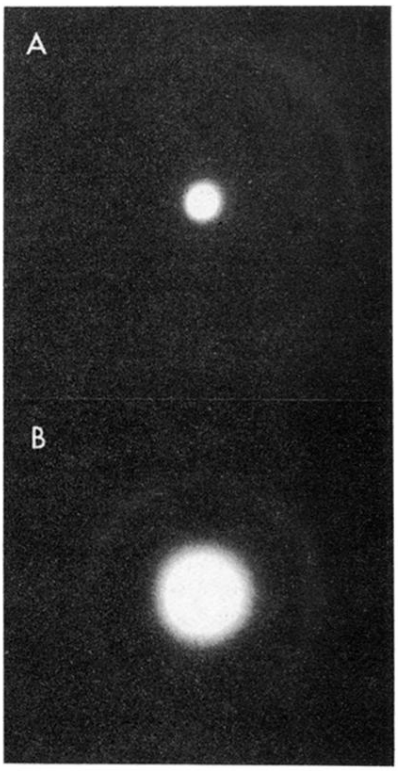

FIG. 8. Transmission electron diffraction patterns for selected regions of micrograph shown in Fig. 7. Regions are indicated in Fig. 7.